Wetting of SiC by Al-Ti alloys and joining by in-situ formation of interfacial $Ti_3Si(Al)C_2$

Valenza Fabrizio[a,*], Gambaro Sofia, Muolo Maria Luigia, Salvo Milena, Casalegno Valentina

[a] National Research Council, Institute of Condensed Matter Chemistry and Technologies for Energy (CNR-ICMATE), Genoa, Italy
Politecnico di Torino, Department of Applied Science and Technology, Corso Duca degli Abruzzi 24, 10129 Torino, Italy
* corresponding author: fabrizio.valenza@ge.icmate.cnr.it

Abstract

Two pressureless and reliable procedures for brazing SiC-based materials have been designed. The joining was obtained by the in-situ formation of a $Ti_3Si(Al)C_2$ MAX phase using simple Al-Ti interlayers. Wettability studies were conducted using several Al-Ti alloys in contact with SiC at 1500°C. The interfacial microstructures and thermodynamic analysis demonstrated that liquid Al_3Ti in contact with SiC formed a well-bonded $Ti_3Si(Al)C_2$ interfacial layer. These findings guided the design of two joining methods: one consisted of the simple infiltration of Al_3Ti into the brazing seam, while an Al_3Ti paste/Ti/Al_3Ti paste interlayer assembly was designed for the second process. Sound interfaces without cracks were obtained in both processes. The average shear strength was very high, 296 MPa, for the infiltration method; the drawback was the presence of residual Al. Joining through Al_3Ti/Ti/Al_3Ti interlayers avoided the presence of low-temperature melting phases, with lower shear strength: 85 or 89 MPa depending on the testing method.

Keywords: Wetting; Brazing; Silicon Carbide; Shear strength

1. Introduction

SiC is a compound of great technological significance, due to its excellent thermal, chemical and mechanical properties. SiC is often used as a matrix or reinforcing phase in ceramic matrix composite materials (e.g. SiC_f/SiC, C_f/SiC, ZrB_2/SiC, etc.) for use in in many high-temperature applications, such as in the aerospace industry, nuclear plants, gas turbines, heat exchangers, automotive components, etc. New joining technologies are increasingly needed to support the very demanding use conditions targeted for these materials, to integrate them in existing structures or to overcome and back-up existing mechanical fastening methods [1]. The design of reliable joints between ceramics is a complex task that requires competences in various scientific and technological fields, such as thermodynamics, surface science and mechanics.

Several conventional diffusion bonding methods are suitable for SiC-based ceramics [2]. However, even though effective, solid-state processes require high temperatures and high pressures to attain a sufficient mass transport; in addition, the surfaces that have to be joined must be meticulously prepared, in order to minimize flaws or voids which could act as strength-limiting defects after processing. These aspects make this technique unreliable in the case of curved surfaces, or when the adjoining surfaces are rough, as in the case of SiC-based composites. In such situations, a liquid-based process is preferable. However, interfacial thermal stresses may arise in conventional brazing methods, due to the expansion and elastic mismatch between the adjoining materials and the brazing seam. Moreover, both degradation of the ceramic phase and interfacial reactions that form brittle interfacial products are aspects that have to be considered when designing brazing processes. The transient liquid phase bonding (TLPB) technique applied to ceramics may overcome these issues [3]. This technique exploits interlayers that are heated up to melting temperatures and wet the seam between the materials being joined, which results in their adhesion and the fabrication of well-bonded, hermetic seals. The starting liquid interlayers give rise to the formation of new phases which, through

chemical interactions and diffusion processes, solidify and homogenize at joining temperatures. This enables their use at temperatures that are potentially well above the joining temperature, provided that the resulting phases comply with the CTEs and the elastic moduli of the joined materials.

Two simple and liquid-based procedures are proposed in this paper with the aim of obtaining reliable SiC to SiC joints, through the in-situ formation of a $Ti_3Si(Al)C_2$ MAX phase, starting from interlayers made of Al and Ti.

Interest in this particular phase arises from its unique combination of metallic and ceramic properties [4], such as its high melting point, oxidation strength, wear and irradiation resistance, as well as its lattice matching with SiC at basal and non-basal planes. In addition, Ti_3SiC_2 has interesting high temperature properties, such as plastic deformation behaviour at temperatures above 1200°C, which can help to comply stresses when the joints are under high temperature stress [5,6].

A Ti_3SiC_2 MAX phase has recently been adopted as a joining medium for SiC in solid state processes, with successful outcomes [7-10]. Dr. Henager's research group at PNNL (the USA) used a Ti_3SiC_2 MAX phase as a joining material and investigated its post irradiation properties [11]; in this case, a composite made of SiC and Ti_3SiC_2 was produced using the displacement reaction between SiC and TiC and a tape casting process was used as a joining technique [12]. More recently, Ti_3SiC_2 has been considered as a joining filler for SiC and CMC materials, but only a few studies are available on this subject [13-16]. A complete review of joints obtained using Ti_3SiC_2 as a joining material is given in [9]: high temperatures and high pressure are required in most of the reviewed joining processes. In all the previously mentioned research activities, the joining processes rely on the reaction between the joining material and the surface that has to be joined. Lower pressures were adopted in [17], where SiC/SiC composites were joined using Ti_3SiC_2 or an Al-based MAX phase, that is, Ti_3AlC_2, as the joining material.

Other works have reported the possibility of joining Ti_3SiC_2 to itself using Al interlayers in a TLPB process [18], Ti_3SiC_2 to Ti_3AlC_2 via diffusion bonding [19] and Ti_3AlC_2 to itself using Si interlayers

in a diffusion bonding process [20]. All these processes are appealing because of the existence of a $Ti_3Si(Al)C_2$ solid solution obtained by means of partial substitution of Si by Al.

This literature information has been combined here to design simple, reliable, pressureless and liquid-based joining processes for SiC-based materials. The main goal was the achievement of robust and reliable SiC/SiC joints through the in-situ formation of a $Ti_3Si(Al)C_2$ phase, starting from simple Al-Ti interlayers. In a similar way to a TLPB process, the in-situ formation of the desired phase at the process temperature would allow to overcome the thermal stresses associated with the solidification of the interfacial phases by cooling over a broad temperature range.

In order to determine the feasibility of the process, to study the interfacial phenomena that occur at the different stages of the joining process and to select the most appropriate composition of the interlayers, wetting experiments were performed using different compositions of Al-Ti in contact with ultra-pure CVD-SiC ceramic substrates. Wetting tests, which measure the contact angle of a liquid lying on a solid, provide information on the distribution of a liquid joining phase at the adherends. The consequent microstructural characterisation and interpretation of the resulting interfaces, through thermodynamic tools, give information on the best process parameters. Given the great technological importance of SiC, a rich literature exists about the wetting and interfacial reactivity of this ceramic by liquid metals and alloys [21-23]. These studies refer also to the wetting of pure Al on SiC [24-27]; according to these results, Al wets SiC, but brittle Al_4C_3 forms at the metal-ceramic interface. Adding a few atomic percent of an active element, such as Ti, improves the wetting and leads to the disappearance of the deleterious Al_4C_3 phase in favour of Ti-rich phases such as TiC [28]. However, to the best of our knowledge, no data are available about the wetting of Al-Ti alloys on SiC for a greater Ti content than 6 at. %.

On the basis of the results of wetting tests, of microstructural characterization and of thermodynamic predictions, two different approaches were designed to join SiC to SiC: in the first one, that is, the infiltration method, the joining medium, Al_3Ti, was left to infiltrate into the gap between the adjoining materials as a result of capillary forces. In the second one, that is, the assembly

method, the SiC surfaces were coated with an Al_3Ti paste, and a 50 µm Ti foil was then sandwiched between the coated ceramic samples.

Finally, these joints were characterized from the microstructural point of view and their mechanical behaviour was critically evaluated by means of shear and torsion tests.

2. Experimental procedure

Wetting tests were conducted in a tubular alumina furnace (T_{max} = 1600°C) that can be used in high vacuum or controlled atmospheres [29]. The metal/ceramic couples were introduced into the preheated furnace, by a magnetically operated push rod, only after the temperature had reached equilibrium; complete melting occurred in ~30 s. After the tests had been completed, the samples were extracted from the hot part of the experimental chamber using the same push rod, and they reached room temperature in ~30 s. A protective atmosphere (Ar/ 5% H_2, static), gettered by Zr foils placed near the samples, was used. This configuration prevented both evaporation and oxidation of the liquid alloys, and allowed clean droplets to form, as analytically demonstrated in a previous work [30]. A CCD camera, connected to acquisition and calculation software, allows the samples to be observed and the contact angles to be measured. The experiments lasted ten minutes and were performed at 1500°C for all the compositions.

In order to obtain reference data from samples that were not contaminated, the wetting tests were performed on commercially available high purity materials and on well-polished ceramic substrates. The minimum purity of the Al (Metalli Preziosi, Milano, I) was 99.9999 at. %. The main impurities (less than one ppm) in the Al were Fe and Ni. The minimum purity of the Ti (Goodfellow, Hungtingdon, UK) was 99.99 at. % and the main impurities (in ppm) were Fe:10, Si: 5, Nb: 5.

The Al-Ti drops that were used for the wetting experiments were prepared by arc melting, combining appropriate amounts of the two elements and remelting the samples five times in order to ensure

homogeneity of their compositions. Arc melting was performed under an Ar atmosphere; before melting the alloys, the oxygen content in the chamber was reduced by arc-melting a piece of Zr.

The wetting experiments were performed on fully dense, ultra-pure (99.9995 at. %) chemically vapour deposited (CVD) SiC substrates (Morgan Advanced Materials, USA). The SiC materials obtained by means of CVD exhibit an FCC (β) crystal structure and a fine grained (<5μm) polycrystalline microstructure. In order to avoid pinning phenomena at the drop triple line, the substrates were polished with a 1 μm diamond paste to reach a surface roughness Sa = 4nm, which was measured using an optical confocal profilometer (Sensofar S-neox) over a 1.75 x 1.32 mm^2 surface area.

The Al-Ti phase diagram calculated by Thermocalc is shown in Figure 1 (data from [31]).The three vertical lines indicate the examined alloy compositions: a) 3at. % Ti, b) 25 at. % Ti, corresponding to the Al3Ti compound and c) 46 at. % Ti, corresponding to the AlTi compound.

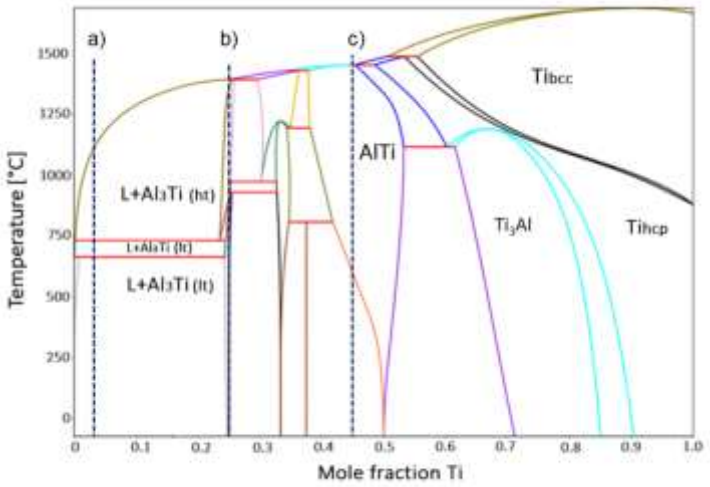

Figure 1: Binary Al-Ti phase diagram with indication of the three compositions: a) Al-Ti 3 at.%, b) Al-Ti 25 at%, c) Al-Ti: 46 at. %.

Two pressureless methods were adopted (Figure 2) to join together sintered 10 x 5 x 3 mm SiC pieces (Frialit SiC 198D, Mannheim, Germany, purity > 98 at. %, open porosity < 3%); in this case, only a rough polishing of the surfaces was done with a 15 μm grit size diamond paste. In the infiltration method, the joining process took place by means of capillary infiltration: a piece of previously melted

Al-Ti alloy, which had been homogenized by arc melting as previously explained, was placed near the adjoining surfaces and left wet to infiltrate between the two materials.

In the assembly method, the following assembly geometry was designed: SiC/Al_3Ti paste/Ti foil/Al_3Ti paste/SiC. A paste was prepared from a mixture of Al_3Ti powder (Goodfellow, Cambridge, the UK, purity: 99 at.%; mean particle size: 45 μm) and α-Terpineol, and then applied to the SiC surfaces by means of slurry coating. The α-Terpineol was allowed to evaporate under a vacuum; the slurry coating process was designed to assure a thickness of between 40 and 60 μm. The coated SiC pieces were then sandwiched together with 50 μm thick Ti foils (Goodfellow, Cambridge, UK, purity > 99.99 %).

In both procedures, the assemblies were introduced into a furnace at 1500°C under a static Ar/H_2 atmosphere; after a holding period of 10 min, the samples were cooled down at 5°C/min.

Some joints were cross-sectioned and polished for a microstructural investigation, while at least 6 samples were used for a mechanical characterization.

The mechanical strength of the joined samples was appraised using a single lap offset shear test. The load was applied by moving the cross-head (equipment: tensile testing machine: Sintech 10/D) at a speed of 0.5 mm/min at room temperature, using a single lap offset (SLO) test under compression, according to a method adapted from the ASTM D905-08 standard and described in [32].

Additional mechanical tests were performed using the torsion test on hourglass shaped adherends, as described in [33]; a custom-made torsion machine with various suitable fixtures and a cross-head speed was used to characterize the joints. The torsion samples were fully joined hourglass shaped SiC samples, obtained by joining two half hourglasses; the designed joined area was 78.5 mm^2.

The samples were tested by means of a method that was based on a modification of the ASTM F734-95 standard, with the aim of obtaining failure under a pure shear state in the bondline subjected to torsion. This method was only used for the joints obtained using method 2; in fact, the infiltration method can produce residual external menisci that could affect the maximum rupture strength.

The maximum force was recorded, and the apparent shear strength was calculated by dividing the maximum force by the joined area (~ 50 mm^2) for SLO or by using the equation reported in [32] for the torsion tests. The fracture surfaces were examined to determine fracture propagation.

Figure 2: a1) scheme of the capillary infiltration assembly; a2) scheme of the infiltration method mechanism; b) scheme of the Al_3Ti-Ti-Al_3Ti paste assembly.

3. Results and discussion

3.1 Wetting and interfacial reactivity

Figure 3 shows the contact angle vs. time plots for each system at 1500°C along with the final contact angles measured after 600 s of liquid-solid contact.

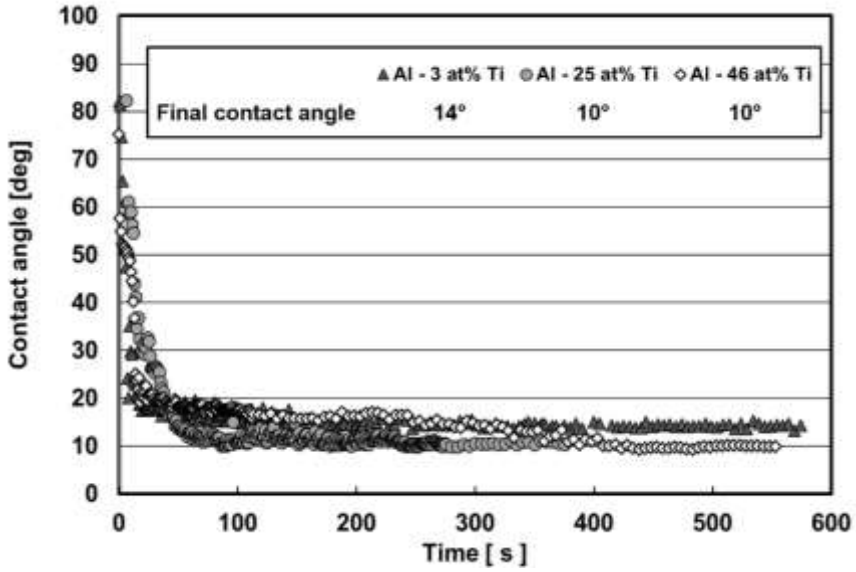

Figure 3: Contact angle vs. time for the Al-Ti alloys in contact with SiC at 1500°C

All the systems exhibited very low contact angles (<< 90°C), which, in principle, would ensure intimate contact between the materials that have to be joined. Very fast kinetics were recorded for all the systems tested at 1500°C, and the final angles were obtained in less than one minute. Figure 4 shows SEM images (back-scattering mode) of the cross-sectioned Al-3 at. % Ti after a wetting test on SiC. The SEM-EDS microstructural observations (Table 1) showed the formation of a TiC layer at the interface that is analogous to similar Al-Ti alloys reported in the literature [28]; a continuous interlayer of the desired phase, $Ti_3Si(Al)C_2$, was not observed. The bulk of the drop was formed by Al and Al_3Ti, coherently with the binary Al-Ti phase diagram.

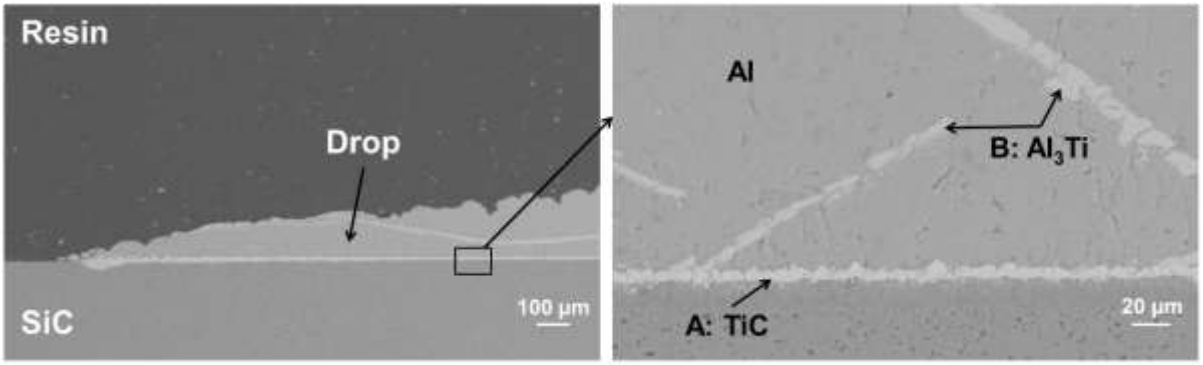

Figure 4: Cross section of the Al – 3 at% Ti alloy after contact with CVD-SiC at 1500°C (BSE image).

Table 1: EDS chemical analysis (at.%) of different regions identified in the wetting samples; at least 5 spots were analyzed for each phase.

Al-Ti drop	Region	Elemental composition (at. %)				Possible phase
		Al	C	Si	Ti	
Al – 3 at% Ti Figure 4	A	1.3	47.3	-	51.4	TiC
	B	63.4	-	7.8	27.6	Al_3Ti
Al – 25 at.% Ti (Al_3Ti) Figure 5	C	5.6	34.4	9.2	50.7	$Ti_3Si(Al)C_2$
	D	0.8	48.6	0.3	50.4	TiC
	E	72.3	-	2.3	25.4	Al_3Ti
	F	94.6		4.2	1.2	Al(Si,Ti)
Al – 46 at.% Ti Figure 6	G	2.3	36.2	13.4	48.1	$Ti_3Si(Al)C_2$
	H	2.7	19.3	27.6	50.4	$Ti_5Si_3C_x$

When the Al-25 at.% Ti composition, which corresponds to the Al_3Ti compound, was used, the formation of a continuous interlayer of $Ti_3Si(Al)C_2$, with a thickness of about 50 µm (Figure 5), was observed on the top of a very thin interlayer of TiC of about 1 µm in contact with SiC. The bulk of the drop was formed by Al_3Ti and Al with Si and dissolved Si and Ti.

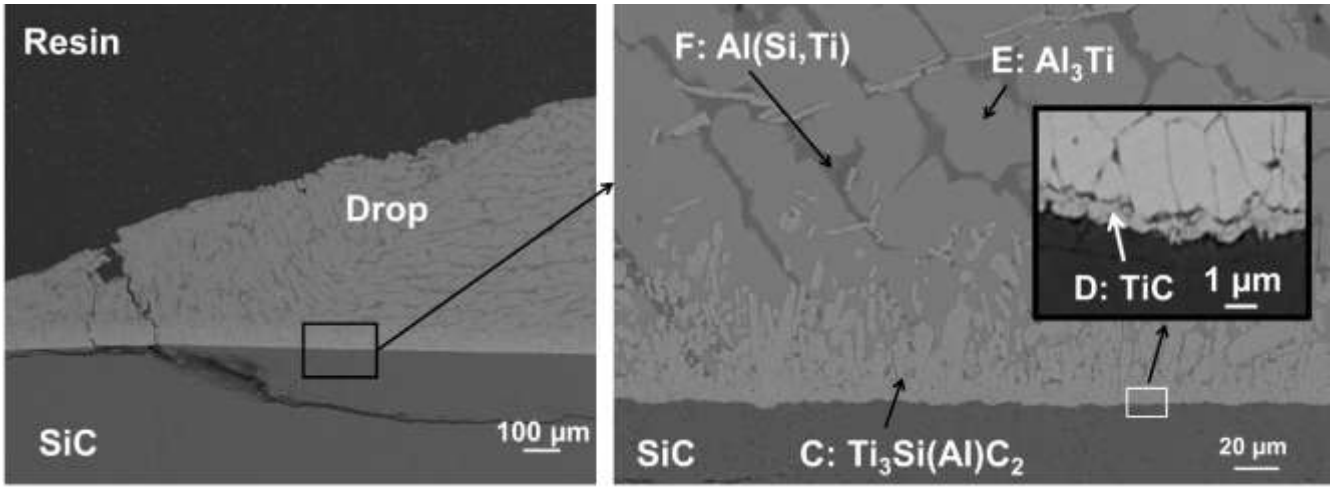

Figure 5: Cross section of the Al – 25 at% Ti alloy after contact with CVD-SiC at 1500°C. The crack is due to the fast cooling of the sample after the test (BSE image).

The SEM-EDS analysis performed on the Al – 46 at. % Ti alloy after contact with CVD-SiC at 1500°C (Figure 6) showed an increased interfacial reactivity and a microstructure, formed by a layer of $Ti_3Si(Al)C_2$, and the presence of the $Ti_5Si_3C_x$ phase in the bulk of the drop and at the metal/ceramic interface. No TiC interlayer was detected at the interface between the ceramic and the Al-Ti alloy. This suggests that the excess of Ti, which gives rise to intermetallic compounds and to an increased reactivity, could be detrimental for joining processes.

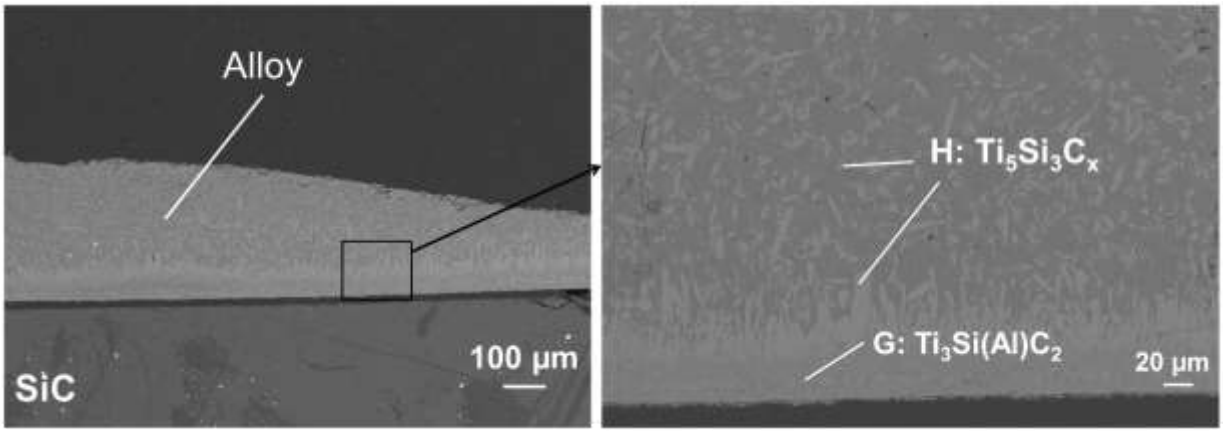

Figure 6: Cross section of the Al – 46 at% Ti alloy after contact with CVD-SiC at 1500°C (BSE image).

The experimental results regarding the high temperature reactivity between the Al-Ti alloys and the silicon carbide show that any discussion on the final equilibrium configurations should be conducted taking Si and C into consideration. In order to foresee the different phase equilibria that occur during the wetting experiments, a specific thermodynamic database has been developed, in which the C, Si, Al and Ti elements have been included. Binary and ternary interaction parameters were first taken from literature assessments (Al-Si, Al-Ti, Al-C, C-Si, C-Ti , Si-Ti , Al-C-Si , Al-C-Ti , Al-Si-Ti , C-Si-Ti [31,34-39]) and subsequently adapted to obtain a self-consistent set of phase models and interaction parameters.

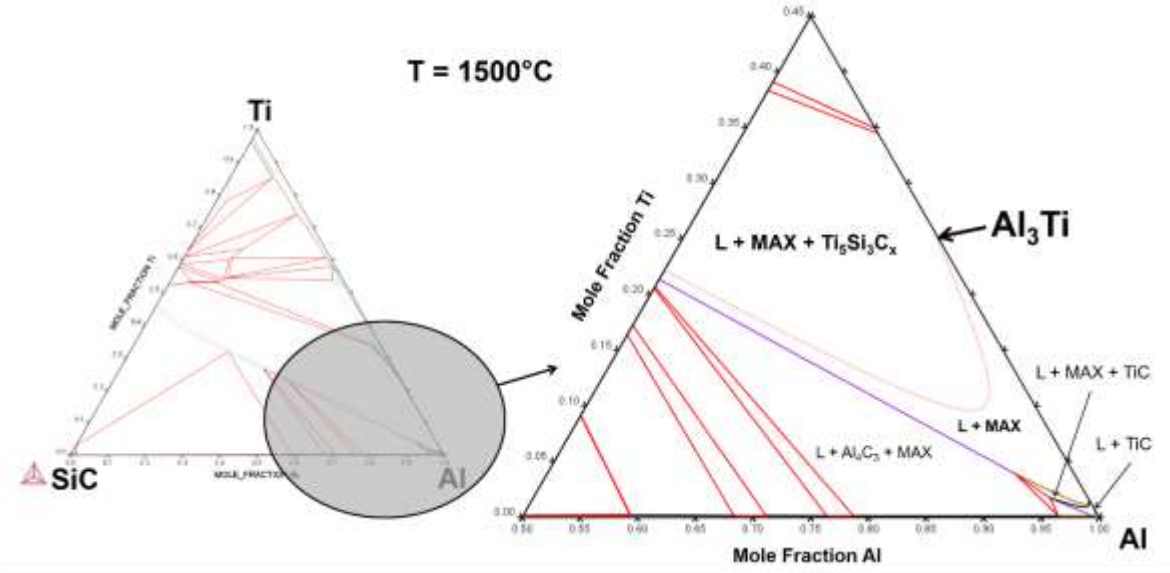

Figure 7 displays an isothermal section of the SiC-Al-Ti phase diagram at 1500°C computed by CALPHAD, using the aforementioned database.

Looking at the Al rich-corner, it can be observed that pure Al in contact with SiC results in the formation of Al_4C_3. When a few atomic percent of Ti are added, the TiC phase forms according to the aforementioned literature [28]. When more Ti is added, equilibrium is established between the liquid and the MAX $Ti_3Si(Al)C_2$ in contact with SiC, as observed for the Al_3Ti/SiC wetting couple. When Ti exceeds 25 at. % in Al, the Ti_5Si_3Cx phase is in equilibrium with a liquid and the MAX phase; the large area that can be observed suggests that a great interfacial reaction can be expected,

as experimentally observed for the Al 46 at. % Ti alloy in contact with SiC. This would result in a great dissolution of the SiC phase and poor mechanical properties.

The main goal of this work is not that of discussing the quaternary Al-C-Si-Ti phase diagram and the cooling behaviour of Al-Ti alloys in contact with SiC in detail, as these aspects will be presented in a forthcoming paper by the same Group. The main finding that is presented here, pertaining to joining processes, is that the microstructural observations of quenched wetting couples and the isothermal section of the SiC-Al-Ti system have demonstrated that the $Ti_3Si(Al)C_2$ phase in fact formed in-situ at 1500°C when liquid Al_3Ti was in contact with SiC, and not during the cooling of the samples.

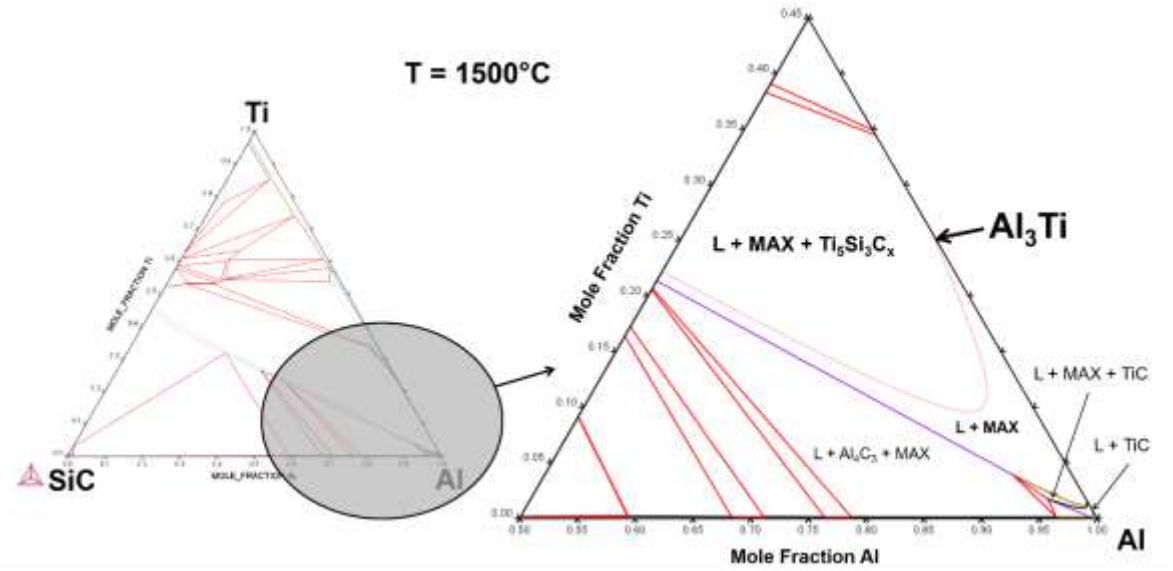

Figure 7: SiC-Al-Ti isothermal section at 1500°C. The picture on the right represents a zoomed view of the Al corner.

Therefore, these wetting results prove the possibility of using Al-Ti interlayers for the joining of SiC-based materials. The Al_3Ti phase in fact ensures contact between the adjoining materials, and the (transient) liquid phase evolves by reaction and diffusion, solidifies at the testing temperature and leads to the $Ti_3Si(Al)C_2$ MAX phase at the interface.

3.2 Joining

On the basis of the results of the wetting tests, the Al-Ti 25 at. % alloy was chosen to obtain a set of joined specimens. As detailed in the experimental procedure section, two different kinds of processes were adopted: 1) joining by capillary infiltration of Al_3Ti inside the seam between adjoining materials; 2) joining by $Al_3Ti/Ti/Al_3Ti$ interlayers. Both procedures offer the advantage of relying on a liquid that wets the adjoining surfaces, fills all the cavities and all the unevenness; as adhesion during the joining process is ensured by capillary forces, no external pressure is necessary.

Moreover, the first procedure has the advantage of being easy to prepare and of being suitable for rough and curved surfaces.

The following picture (Figure 8) shows the cross-section of a SiC-SiC joint obtained by capillary infiltration of Al_3Ti at 1500°C for 10 minutes. The joined region, which was formed after the infiltration of the brazing alloy, had a thickness of about 30 microns and contained the following phases (Table 2): large $Ti_3Si(Al)C_2$ grains, small TiC grains and the Al_3Ti phase, in agreement with the wettability tests results. In addition, a few Al spots, which can be detrimental from the point of view of high-temperature applications, were detected. A perfect infiltration was obtained, and the adhesion between the braze and SiC seems to have been successful: no macro-cracks or gaps were observed along the joined region. The infiltrated joining material acts as a “grip” embedded within the SiC surface. In fact, this joining filler appears to be a good joining material candidate for CMC, as well as for bulk ceramics: it can be used to effectively heal surface cracks that formed during the manufacturing of the coating of a CMC (i.e. SiC/SiC coated by CVD-SiC) or to penetrate into the porosity of a CMC.

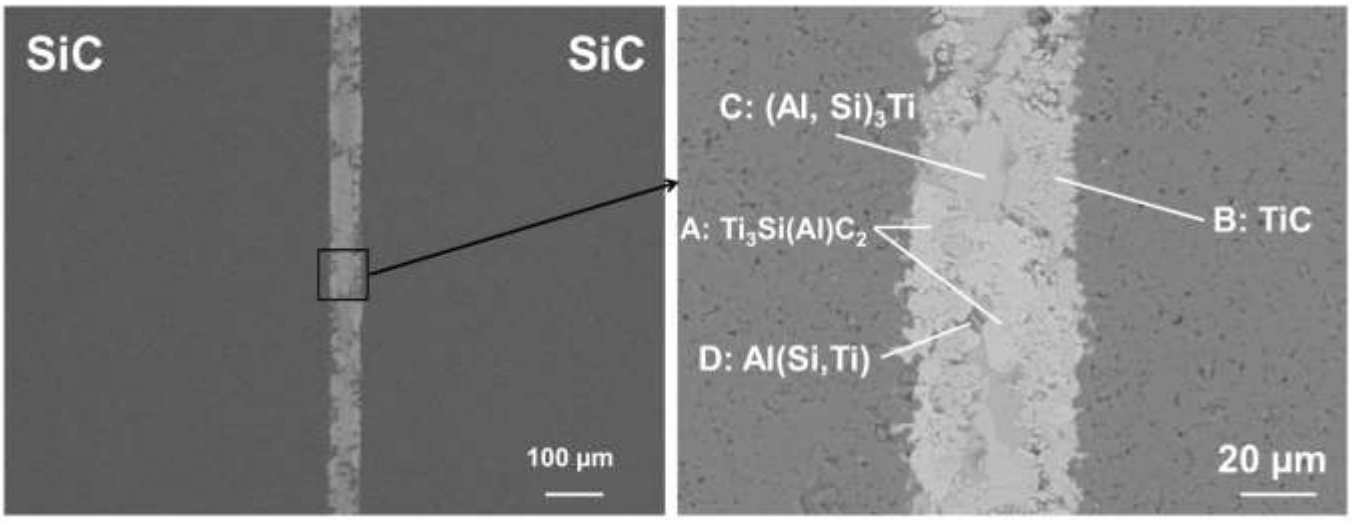

Figure 8: cross-section of a SiC-SiC joint obtained by capillary infiltration of Al_3Ti at 1500°C (BSE image)

Table 2: EDS chemical analysis (at.%) of different regions identified in joined samples; at least 5 spots were analyzed for each phase.

Type of joining	Region	Elemental composition (at. %)				Possible phase
		Al	C	Si	Ti	
Capillary infiltration of Al_3Ti Figure 8	A	1.1	31.0	14.8	53.1	$Ti_3Si(Al)C_2$
	B	0.1	46.9	0.2	52.8	TiC
	C	57.0	3.6	12.5	26.9	$(Al,Si)_3Ti$
	D	91.6	6.2	1.6	0.6	Al(Si,Ti)
Al_3Ti paste/Ti foil/Al_3Ti paste Figure 9	E	59.0	2.9	10.8	27.3	$(Al, Si)_3Ti$
	F	0.5	32.6	15.1	51.8	$Ti_3Si(Al)C_2$
	G	11.1	-	55.1	33.8	τ_2

In order to increase the expected service temperature, by eliminating any residual Al and increasing the amount of interfacial MAX phase, in the assembly method Ti was added, in the form of 50 µm

thick foils sandwiched between two SiC pieces previously coated with a Al_3Ti paste. In this case, the use of capillary infiltration was not possible, because the infiltrating alloy would have more likely reacted with Ti and would not have completely filled the brazing gap. Figure 9 shows an example of the obtained microstructure. The thickness of the obtained brazing seam is about 150 µm. As the paste had a thickness of 40-60 µm for both of the adherends, and the Ti interlayer had a thickness of 50 µm, no significant loss of material occurred during the process. A microstructural examination showed the presence of the $Ti_3Si(Al)C_2$ phase at the interface with SiC and interspersed in the brazing seam; the other phases were: the Al_3Ti phase, with Si substituting Al up to 10 at%, and a phase identified as the τ_2 phase in the Al-Si-Ti phase diagram (Al: 13; Si: 53; Ti: 34 at. %), which, at this composition, melts incongruently at 1338°C [40]. No Al pockets were found for this process.

Regardless of which joining process is considered, that is, infiltration or assembly, all the interfaces between the ceramic and the joining material are continuous, and there are no detectable cracks at the joining interface.

The good joining results demonstrate that using a liquid medium to ensure adhesion between SiC allows a specific surface preparation to be avoided, contrary to what was reported in [13], where polishing of the facing surface was considered mandatory to optimize the contact area and reduce roughness.

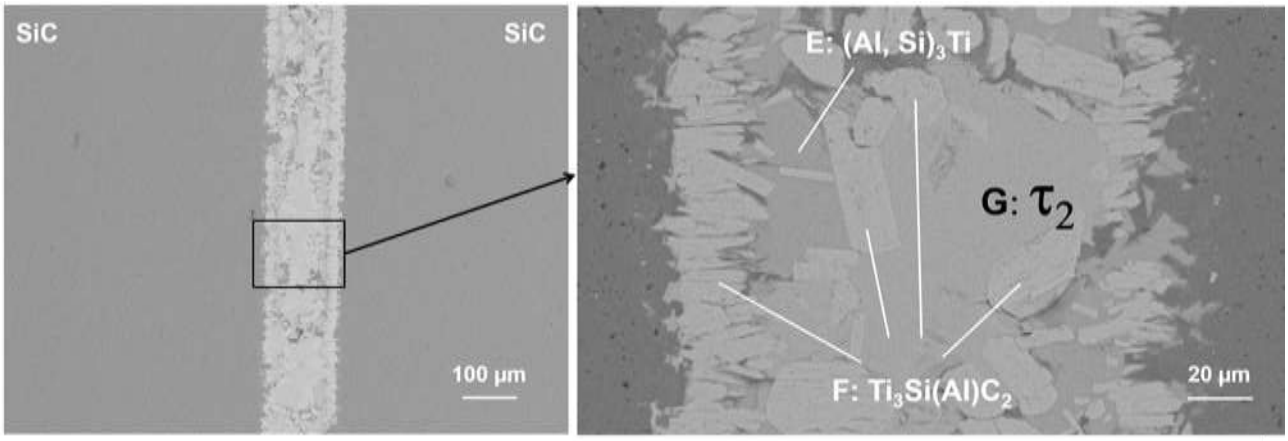

Figure 9: cross-section of a SiC-SiC joint obtained from the Al_3Ti/Ti/Al_3Ti assembly (BSE image)

Table 3: summary of the main features of the obtained joints

Joining method	Resulting phases	Thickness [μm]	Shear strength [MPa]	Crack propagation
Al_3Ti infiltration	$Ti_3Si(Al)C_2$, Al_3Ti, Al, TiC	50	296 ± 20 (SLO test)	Mixed mode (SiC + interlayer)
Al_3Ti paste / Ti / Al_3Ti paste	$Ti_3Si(Al)C_2$, $(Al, Si)_3Ti$, τ_2 Al-Si-Ti	150	85 ± 9 (SLO test) 89 ± 11 (Torsion test)	Mixed mode (SiC + interlayer)

3.3 Mechanical characterization

Several specimens, produced by the two joining methods, were used for mechanical tests.

The average shear strength measured in the single lap offset (SLO) shear test for the joints obtained by means of capillary infiltration was 296 ± 20 MPa, while it was 85 ± 9 MPa and 89 ± 11 MPa for the SLO and the hourglass torsion test, respectively, for the joints obtained by means of the assembly method (see Table 3). As a general comment, these strength values are very high, compared with those reported in the papers cited in the introduction for the first method, while they are in average for the second one; it is worth noting that the thickness of the joint region is in this case very different in the two cases, as a result of the different joining methods that were adopted. Furthermore, the high mechanical strength could also be attributed to the infiltration of the joining material inside the uneven adherent surfaces, which resulted in an interlocking bonding at the interfaces. The results show that the shear strength of the joined couple obtained by means of the first method depends on the infiltration of the joining filler into the surface roughness in the SiC, which allows the filler to be more uniformly integrated with the substrate over the entire interface.

Visual observations of the samples obtained with the capillary infiltration method showed that the adherents did not detach completely at the end of the test; fractures were located both in SiC and throughout the brazing seam. The pictures in Figure 10 show typical features of the fracture surfaces after the SLO test. Figure 10c shows the formation of kink bands in the $Ti_3Si(Al)C_2$ phase, which are a characteristic feature of this phase related to its plasticity at room temperature [41]. This indicates

the large amount of energy that has to be applied to break this joint, as also indicated by the transgranular fractures observed in the interfacial TiC grains (Figure 10d). Moreover, as shown in Figure 10e, the residual Al inside the joining area, even though detrimental for high-temperature applications, acts as ductile spots; since the amount of observed Al in the microstructure is very low, the plastic deformation in these small spots is not reflected in the load-displacement curve.

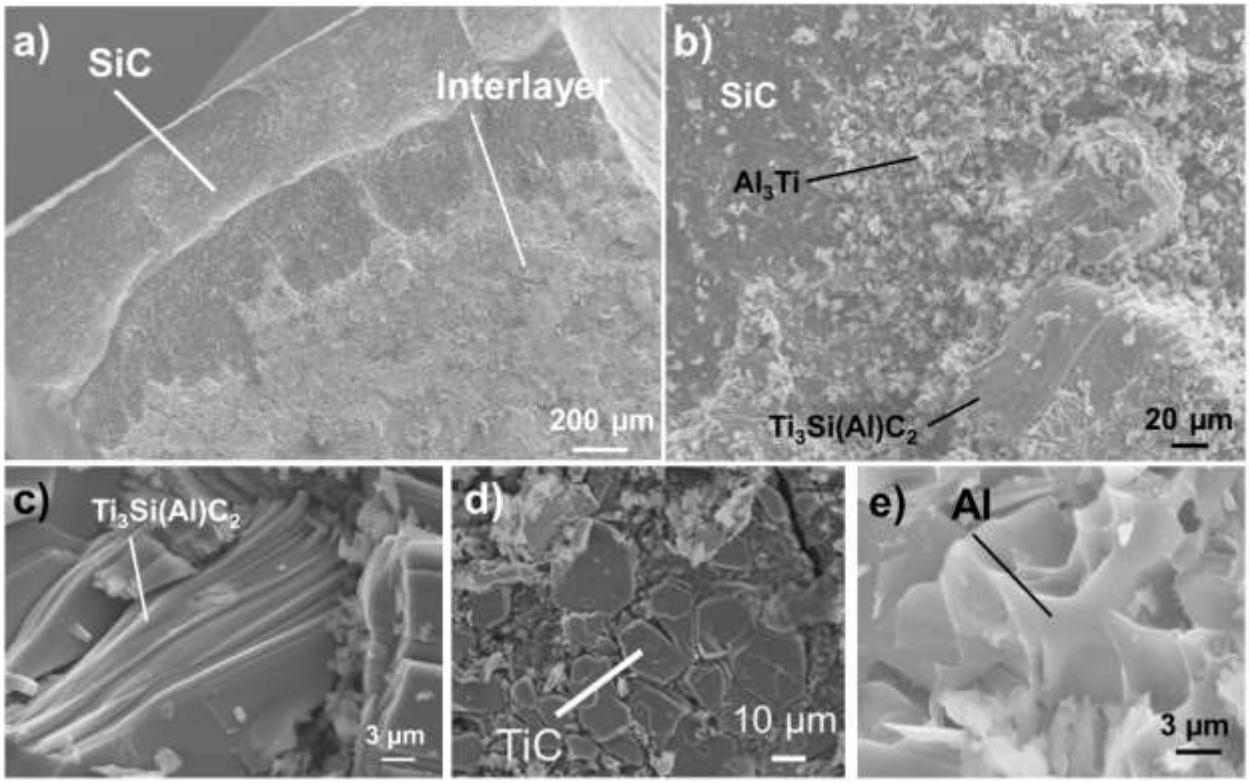

Figure 10: fracture surface of a SiC/SiC joint obtained by capillary infiltration after a shear test. a)-b) macroscopic views of the fractured surface; c) $Ti_3Si(Al)C_2$; d) transgranular fracture in TiC grains; e) plastic deformation in Al spots.

The shear tests on joints obtained from the Al_3Ti paste + Ti interlayer were conducted by means of SLO test and, in order to increase the reliability of the mechanical data, by means of the torsion test. Although the assembly of joined specimens with a miniaturized hourglass geometry is more complicated and this test is unreliable for the capillary infiltration method, it allows the samples to be loaded exactly at the interface.

The picture in Figure 11 shows the polished surface of a joint obtained with the second method after the SLO test. The fracture paths were mainly found in two regions: through the τ_2 phase, located in the middle of the joint, and in the bulk SiC; at the same time, the $Ti_3Si(Al)C_2$/SiC interface is nearly almost completely intact. This indicates not only that the weak point of the joint is the interfacial τ_2 phase (which is absent in the joints produced by infiltration), but also that the thermal stresses that arise during cooling have weakened the SiC base material, which breaks at values well below those measured for the joints obtained via capillary infiltration. The observation of samples broken by torsion confirms that the rupture takes place mainly in the middle of the joints, in correspondence to the τ_2 interlayer.

One of the most critical steps in any kind of joint is the mismatching between the thermal expansion coefficient (CTE) and the elastic moduli between the adherends and the interlayers; these values are summarized in Table 4. Despite the absence of CTE data for $Ti_3Si(Al)C_2$, the results that report the joining of Ti_3SiC_2 by TLPB using Al interlayers [18], suggest values that are close to those of the Ti_3SiC_2 MAX phase. Considering these data, a significant thermal mismatch emerges exists between SiC and $Ti_3Si(Al)C_2$; however, according to the previous literature [8], the plastic behaviour of the MAX phase at room and high temperatures gives compliance during the high temperature process. In addition, for the joints obtained by means of capillary infiltration, the thin TiC interlayer may help to reduce the thermal stress between SiC and the MAX $Ti_3Si(Al)C_2$ phase by virtue of its intermediate CTE value, which leads to the very good mechanical resistance that has been observed.

No data were found in literature for the τ_2 phase, which resulted to be the weak point in the joints obtained through the Al_3Ti/Ti/Al_3Ti assembly. However, the nature of this ternary phase, which has a $ZrSi_2$-type crystal structure and is in fact a $TiSi_2$ phase that has been stabilized to lower temperatures by Al-substitution [40], suggests its brittle nature.

Table 4: thermo-mechanical properties of the compounds considered involved in this work

Compound	Melting point [°C]	Density [g/cm^3]	CTE [10^{-6}/°C]	Young's modulus [GPa]	Source
Al_3Ti	1396	3.3	3.9-4.2	166	[42]
SiC	-	3.21	4.70	440	[43]
Ti_3SiC_2	3200	4.52	8.87	322	[44]
$Ti_3Si(Al)C_2$	-	4.47	-	312	[45]
TiC	3067	4.92	7.40	439	[43]

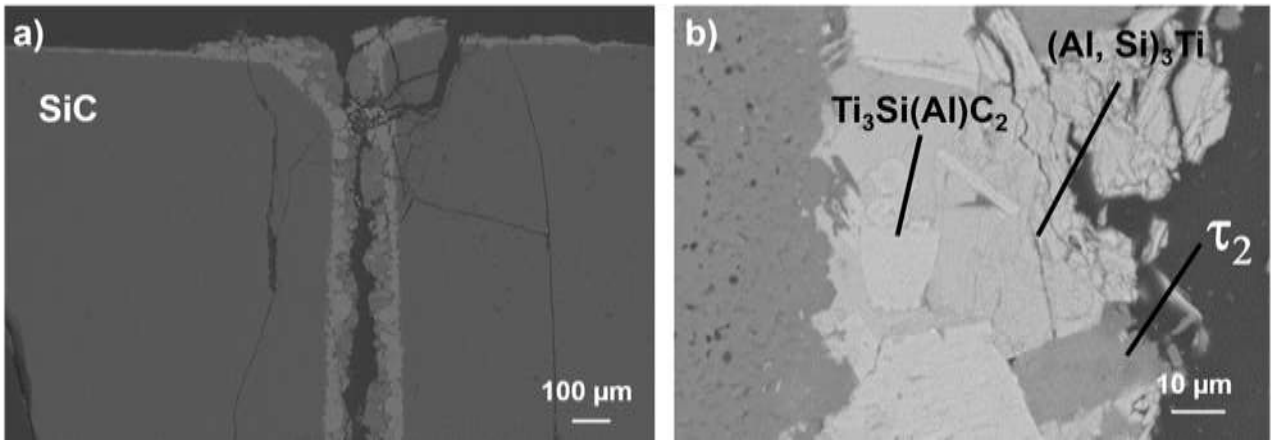

Figure 11: cross section at low (a) and high (b) magnification of a SiC/Al_3Ti/Ti/Al_3Ti/SiC joined sample after a shear test. The observed plain is perpendicular to the applied load (BSE image).

4. Conclusions

The in-situ formation of the $Ti_3Si(Al)C_2$ MAX phase by means of Al-Ti interlayers has been adopted, as part of the topic pertaining to the joining of SiC-based materials for high temperature applications, to obtain reliable SiC-SiC joints. The wetting of SiC by Al-3 at. % Ti, Al-25 at. % Ti and Al-46 at. % Ti was studied at 1500°C. All the studied systems exhibited good wetting; the contact angles ranged from 10 to 14°, and the kinetics lasted less than 100 s. The microstructural examination and an analysis of a specific section of the Al-C-Si-Ti phase diagram demonstrated that the liquid Al-25 at. % alloy (Al_3Ti) formed interfacial $Ti_3Si(Al)C_2$ at the tested temperatures when in contact with SiC.

These findings were used to design two simple and pressureless processes aimed at joining SiC to SiC at 1500°C. In the first method, an Al_3Ti alloy was left to infiltrate between the adjoining surfaces; in the second method, the joints were obtained by covering each surface that had to be joined with an Al_3Ti paste and then sandwiching a Ti foil between them. Sound interfaces were obtained in both processes without any visible cracks. The first method resulted in an interface that was formed by $Ti_3Si(Al)C_2$, Al_3Ti, TiC and residual spots of Al, which are deleterious for high temperature applications. Single lap offset tests showed a very high shear strength of 296 ± 20 MPa. The second method resulted in an interface formed by $Ti_3Si(Al)C_2$, $(Al, Si)_3Ti$ and a phase that was later identified as the τ_2 phase in the ternary Al-Si-Ti system. Single lap offset tests showed an average shear strength of 85 ± 9 MPa; mechanical tests by torsion on hourglass shaped specimens showed an average shear strength of 89 ± 11 MPa.

Owing to its simplicity, the capillary infiltration process may be suitable for the mass production of components, for non-flat components or for rough surfaces, i.e. the typical ones of SiC-based composites; the second method may be suitable when higher service temperatures are expected.

Acknowledgments

The research leading to these results has received funding from the European Union's Seventh Framework Programme FP7 2007-2013 under grant agreement 609188, as part of the European ADMACOM (Advanced manufacturing routes for metal/composite components for aerospace, www.admacomproject.eu) project. Dr. A. Passerone (CNR-ICMATE) is gratefully acknowledged for the fruitful suggestions and discussions. The authors are deeply thankful to S. De La Pierre Des Ambrois (Politecnico di Torino) for the mechanical characterization by torsion tests.

References

[1] M. Ferraris, V. Casalegno, Integration and joining of ceramic matrix composites, Ceram. Matrix Compos. Mater. Model. Technol. (2015) 551–567.

[2] M.I. Osendi, P. Miranzo, Joining methods for hard ceramics, in: Compr. Hard Mater. Vol. 2, Elsevier Ltd., 2014: pp. 231–262.

[3] S.M. Hong, C.C. Bartlow, T.B. Reynolds, J.T. McKeown, A.M. Glaeser, Ultrarapid transient-liquid-phase bonding of Al_2O_3 ceramics, Adv. Mater. 20 (2008) 4799–4803.

[4] M.W. Barsoum, The MAX phases : a new class of solids, Prog. Solid State Chem. 28 (2000) 201–281.

[5] T. El-Raghy, M.W. Barsoum, A. Zavaliangos, S.R. Kalidindi, Processing and mechanical properties of Ti_3SiC_2: II , effect of grain size and deformation temperature, J. Am. Ceram. Soc. 60 (1999) 2855–2860.

[6] M. Radovic, M.W. Barsoum, J. Seidensticker, S. Wiederhorn, Tensile properties of Ti_3SiC_2 in the 25-1300°C temperature range, Scan. Electron Microsc. 48 (2000) 453–459.

[7] P. Tatarko, S. Grasso, T.G. Saunders, V. Casalegno, M. Ferraris, M.J. Reece, Flash joining of CVD-SiC coated C_f/SiC composites with a Ti interlayer, J. Eur. Ceram. Soc. 37 (2017) 3841–3848.

[8] P. Tatarko, A. Mahajan, V. Casalegno, M.J. Reece, T.G. Saunders, I. Dlouh, High temperature properties of the monolithic CVD-SiC materials joined with a pre-sintered MAX phase Ti_3SiC_2 interlayer via solid-state diffusion bonding, J. Eur. Cer. Soc. 37 (2017) 1205–1216.

[9] P. Tatarko, V. Casalegno, C. Hu, M. Salvo, M. Ferraris, M.J. Reece, Joining of CVD-SiC coated and uncoated fibre reinforced ceramic matrix composites with pre-sintered Ti_3SiC_2 MAX phase using spark plasma sintering, J. Eur. Ceram. Soc. 36 (2016) 3957–3967.

[10] C. Jiménez, K. Mergia, M. Lagos, P. Yialouris, I. Agote, V. Liedtke, S. Messoloras, Y. Panayiotatos, E. Padovano, C. Badini, C. Wilhelmi, G. Barcena, Joining of ceramic matrix composites to high temperature ceramics for thermal protection systems, J. Eur. Cer. Soc. 36 (2016) 443–449.

[11] B.N. Nguyen, C.H. Henager, R.J. Kurtz, Modeling thermal and irradiation-induced swelling effects on the integrity of Ti_3SiC_2/SiC joints, J. Nucl. Mater. 495 (2017) 504–515.

[12] C.H. Henager, R.J. Kurtz, Low-activation joining of SiC/SiC composites for fusion applications, J. Nucl. Mater. 417 (2011) 375–378.

[13] S. Grasso, P. Tatarko, S. Rizzo, H. Porwal, C. Hu, Y. Katoh, M. Salvo, M.J. Reece, M. Ferraris, Joining of β-SiC by spark plasma sintering, J. Eur. Ceram. Soc. 34 (2014) 1681–1686.

[14] H. Dong, S. Li, Y. Teng, W. Ma, Joining of SiC ceramic-based materials with ternary carbide Ti_3SiC_2, Mater. Sci. Eng. B. 176 (2011) 60–64.

[15] X. Zhou, H. Yang, F. Chen, Y.H. Han, J. Lee, S. Du, Q. Huang, Joining of carbon fiber reinforced carbon composites with Ti_3SiC_2 tape film by electric field assisted sintering technique, Carbon N. Y. 102 (2016) 106–115.

[16] X. Zhou, Y.H. Han, X. Shen, S. Du, J. Lee, Q. Huang, Fast joining SiC ceramics with Ti_3SiC_2 tape film by electric field-assisted sintering technology, J. Nucl. Mater. 466 (2015) 322–327.

[17] A. Septiadi, P. Fitriani, A.S. Sharma, D. Yoon, Low pressure joining of SiC_f/SiC composites using Ti_3AlC_2 or Ti_3SiC_2 MAX phase tape, J. Korean Ceram. Soc. 54 (2017) 340–348.

[18] X.H. Yin, M.S. Li, Y.C. Zhou, Microstructure and mechanical strength of transient liquid phase bonded Ti_3SiC_2 joints using Al interlayer, J. Eur. Ceram. Soc. 27 (2007) 3539–3544.

[19] X. Yin, M. Li, J. Xu, J. Zhang, Y. Zhou, Direct diffusion bonding of Ti_3SiC_2 and Ti_3AlC_2, Mater. Res. Bull. 44 (2009) 1379–1384.

[20] X.H. Yin, M.S. Li, T.P. Li, Y.C. Zhou, Diffusion bonding of Ti_3AlC_2 ceramic via a Si interlayer, J. Mater. Sci. 42 (2007) 7081–7085.

[21] G.W. Liu, M.L. Muolo, F. Valenza, A. Passerone, Survey on wetting of SiC by molten metals, Ceram. Int. 36 (2010) 1177–1188.

[22] K. Nogi, K. Ogino, Wettability of SiC by Liquid Pure Metals, Trans. Japan Inst. Metals 29 (1988) 742–747.

[23] P. Nikolopoulos, S. Agathopoulos, G.N. Angelopoulos, A. Naoumidis, H. Grübmeier, Wettability and interfacial energies in SiC-liquid metal systems, J. Mater. Sci. 27 (1992) 139–145.

[24] V. Laurent, C. Rado, N. Eustathopoulos, Wetting kinetics and bonding of A1 and A1 alloys on u-SiC, J. Mater. Sci. 205 (1996).

[25] P. Shen, Y. Wang, L. Ren, S. Li, Y. Liu, Q. Jiang, Influence of SiC surface polarity on the wettability and reactivity in an Al/SiC system, Appl. Surf. Sci. 355 (2015) 930–938.

[26] X.S. Cong, P. Shen, Y. Wang, Q. Jiang, Wetting of polycrystalline SiC by molten Al and Al-Si alloys, Appl. Surf. Sci. 317 (2014) 140–146.

[27] X. Fang, T. Fan, D. Zhang, Work of adhesion in Al/SiC composites with alloying element addition, Metall. Mater. Trans. A Phys. Metall. Mater. Sci. 44 (2013) 5192–5201.

[28] N. Sobczak, Effects of Ti on wettability and interfaces in Al/ceramic systems, Charact. Control Interfaces High Qual. Adv. Mater. 9 (2005) 83–91.

[29] F. Valenza, M.L. Muolo, A. Passerone, Wetting and interactions of Ni- and Co-based superalloys with different ceramic materials, J. Mater. Sci. 45 (2010) 2071–2079.

[30] F. Valenza, M. Muolo, A. Passerone, A. Glaeser, Wetting and interfacial phenomena in relation to joining of alumina via Co/Nb/Co interlayers, J. Eur. Ceram. Soc. 33 (2013) 539–547.

[31] V.T. Witusiewicz, A. A. Bondar, U. Hecht, S. Rex, and T. Y. Velikanova, The Al–B–Nb–Ti system III. Thermodynamic re-evaluation of the constituent binary system Al–Ti, J. Alloys Compd., 465(1–2) (2008) 64–77.

[32] A. Ventrella, M. Salvo, M. Avalle, M. Ferraris, Comparison of shear strength tests on AV119 epoxy-joined ceramics, J. Mater. Sci. 45 (2010) 4401–4405.

[33] L. Goglio, M. Ferraris, Bonding of ceramics: An analysis of the torsion hourglass specimen, Int. J. Adhes. Adhes. 70 (2016) 46–52.

[34] S. Gambaro, F. Valenza, M.L. Muolo, A. Passerone, G. Cacciamani, Wettability of SiC and graphite by Co–Ta alloys: evaluation of the reactivity supported by thermodynamic calculations, J. Mater. Sci. 52(23) (2017) 13414-13426.

[35] J. Grobner, H. L. Lukas, and F. Aldinger, Thermodynamic of the Ternary System P3Magl, Calphad, 20(2) (1996) 247–254.

[36] J. Gröbner, H. L. Lukas, and F. Aldinger, 'Thermodynamic calculations in the YAlC system', J. Alloys Compd., 220(1–2) (1995) 8–14.

[37] V. T. Witusiewicz, B. Hallstedt, A. A. Bondar, U. Hecht, S. V. Sleptsov, T. Y. Velikanova, Thermodynamic description of the Al-C-Ti system. J. Alloys Compd. 623 (2015) 480–496.

[38] H. Seifert, Thermodynamic Optimization of the Ti-Si System. Z. Met., 87 (1996) 2–13.

[39] Y. Du, J. C. Schuster, H. J. Seifert, and F. Aldinger, Experimental Investigation and Thermodynamic Calculation of the Titanium-Silicon-Carbon System, J. Am. Ceram. Soc. 83(1) (2000) 197–203.

[40] S. Liu, F. Weitzer, J.C. Schuster, N. Krendelsberger, Y. Du, On the reaction scheme and liquidus surface in the ternary system Al-Si-Ti, Int. J. of Mater. Res., 99(7) (2008) 705-711.

[41] M.W. Barsoum, L. Farber, T. El-Raghy, Dislocations, kink bands, and room-temperature plasticity of Ti_3SiC_2, Metall. Mater. Trans. A. 30 (1999) 1727–1738.

[42] G. E. Totten, D. S. MacKenzie, Handbook of Aluminum: Volume 2. CRC Press, Boca Raton, Florida, USA, 2003

[43] J. F. Shackelford, Y-H Han, S. Kim, S-H Kwon, CRC Materials science and Engineering Handbook, 4th ed. CRC Press, Boca Raton, Florida, USA, 2016

[44] H.B. Zhang, Y.W. Bao, Y.C. Zhou, Current status in Layered Ternary Carbide Ti_3SiC_2, a Review, J. Mater. Sci. Technol. 25(1) (2009) 1-38

[45] D.T. Wan, Y.C. Zhou, Y.W. Bao, C.K. Yan, In situ reaction synthesis and characterization of $Ti_3Si(Al)C_2$/SiC composites, Ceram Int, 32(8) (2006) 883-890